

# Temporal variability of oceanic $\text{CO}_2$ uptake

$F\text{CO}_2$  is set by  $\Delta p\text{CO}_2 = p\text{CO}_2 - p\text{CO}_{2,\text{atm}}$

... and given the well-known atmospheric  $\text{CO}_2$  concentration we here identify seawater  $p\text{CO}_2$  discrepancies between state-of-the-art CMIP6 models and gridded  $p\text{CO}_2$ -products (SeaFlux, Fay et al., 2021).

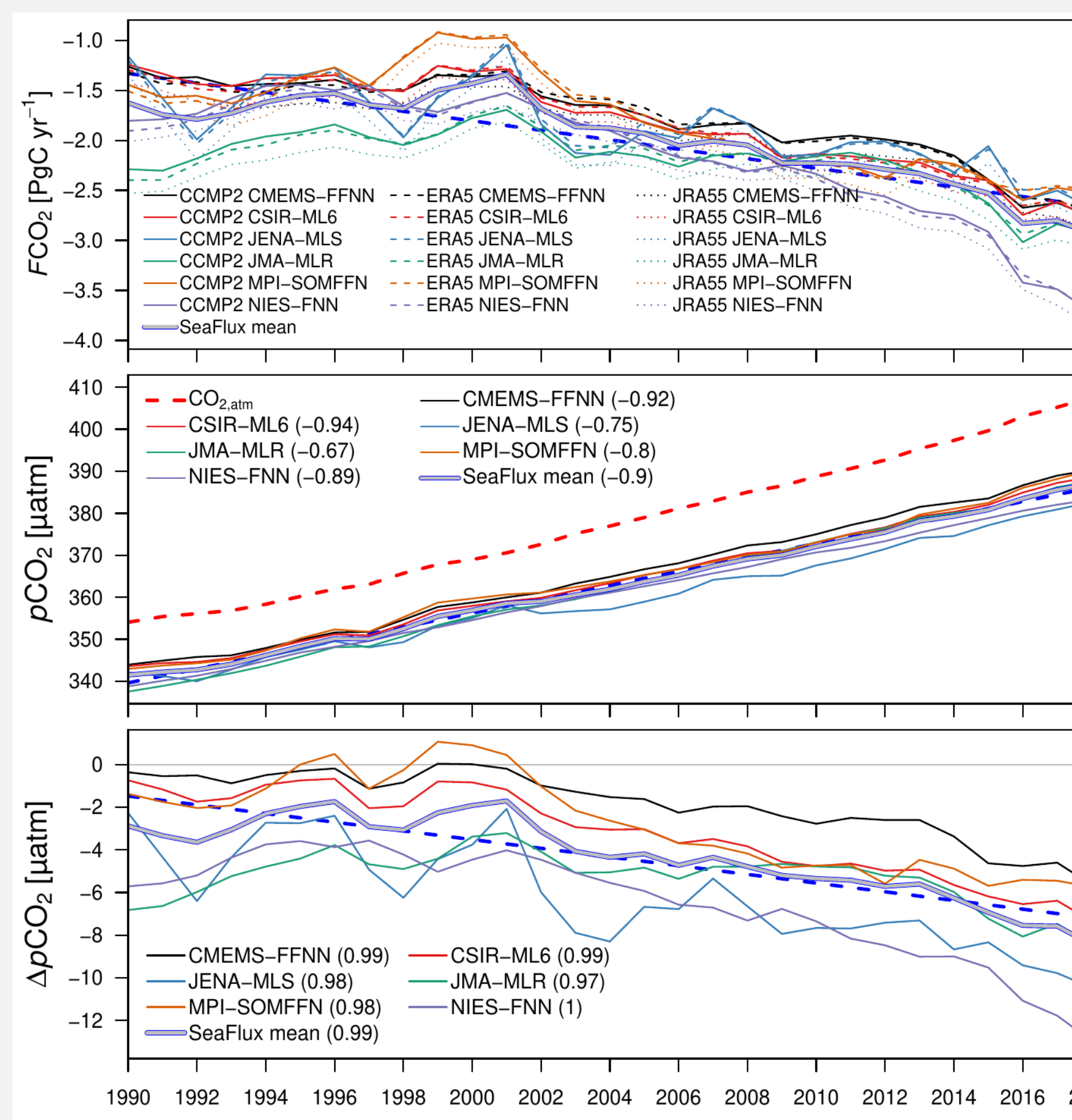
This is of importance since the ocean takes up ~25% of anthropogenic emissions since 1850 (Friedlingstein et al., 2023).

In addition to available CMIP6 data, we here present results from the global coupled climate model

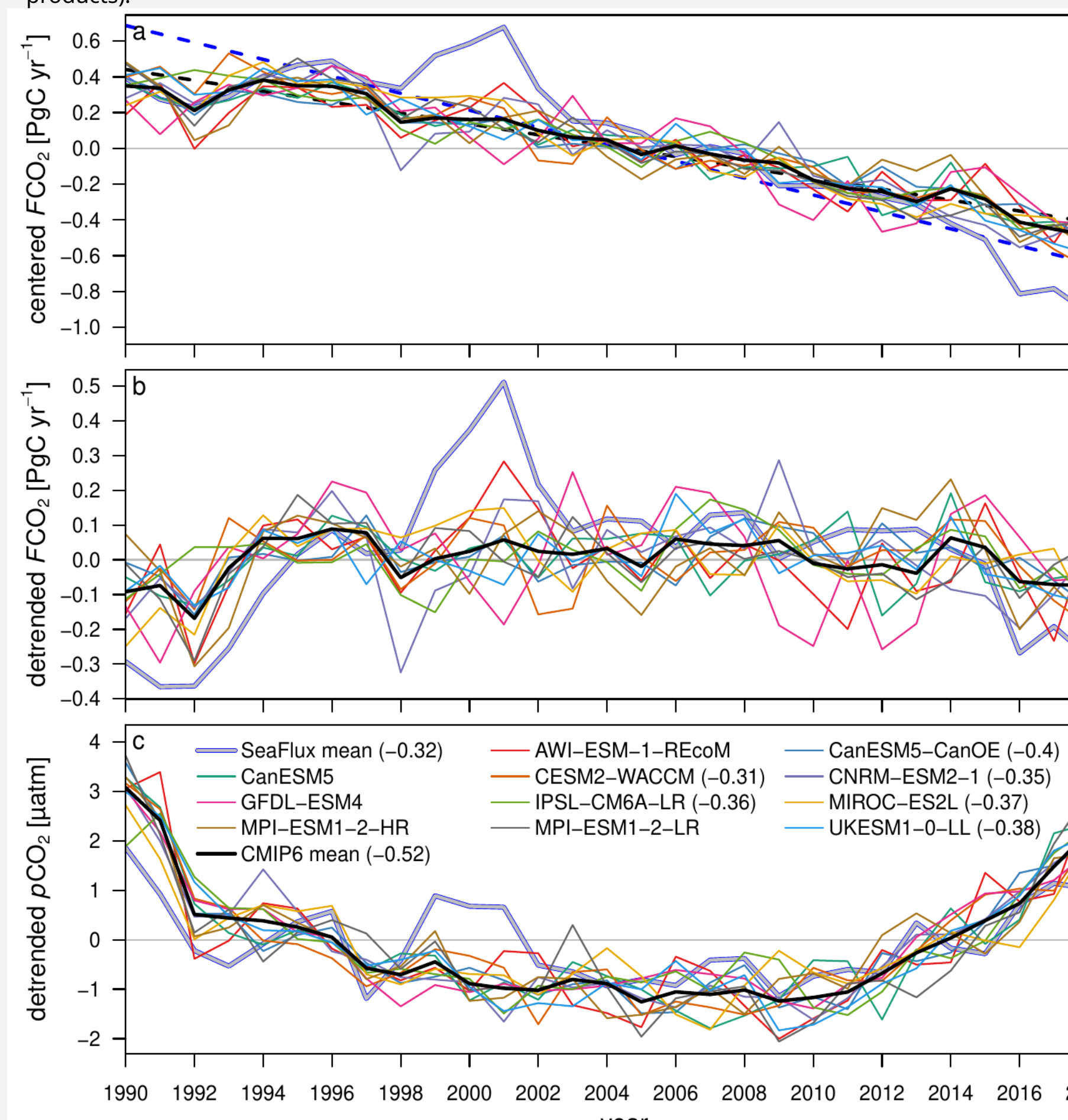
AWI-ESM-1-REcOm that simulates atmosphere, ocean and sea ice physics as well as the ocean biogeochemistry with the Regulated Ecosystem Model version 2 (REcOM; Hauck et al., 2013; Schouren-Kristensen et al., 2014).

**REcOM**  
Regulated  
Ecosystem Model

Temporal  $p\text{CO}_2$  variability is obtained by detrending globally and regionally averaged time series, i.e. removing their linear temporal trends (e.g. DeVries, 2022).



↑ Annual mean globally integrated  $F\text{CO}_2$  (a) and averaged  $p\text{CO}_2$  (b) and  $\Delta p\text{CO}_2$  (c) from SeaFlux (Gregor and Fay, 2021), thick gray-blue line is ensemble mean, thick dashed blue line is linear trend of ensemble mean. In a, negative values denote oceanic  $\text{CO}_2$  uptake and labels refer to wind and  $p\text{CO}_2$ -products. In b, the red dashed line is the globally averaged observed atmospheric  $\text{CO}_2$  mole fraction (in ppm; Lan et al., 2023). Numbers in labels in b and c provide significant correlations with a (averaged over three wind products).



↑ Detrended annual mean  $p\text{CO}_2$  from SeaFlux ensemble mean (Gregor and Fay, 2021) and CMIP6 models averaged globally (a) and over five biomes (map in a; Gregor et al., 2019). Positive values mark years with higher  $p\text{CO}_2$  compared to the linear trend. Numbers in labels after 'C' and 'N' provide correlations with detrended annual global mean atmospheric  $\text{CO}_2$  concentration (dashed red line) (identical in all panels, Lan et al., 2023) and annual mean Niño 3.4 anomaly index (Rayner, 2003), if significant. In b, red/blue bars mark El Niño/La Niña events (Niño 3.4 index area shown by black box in map).

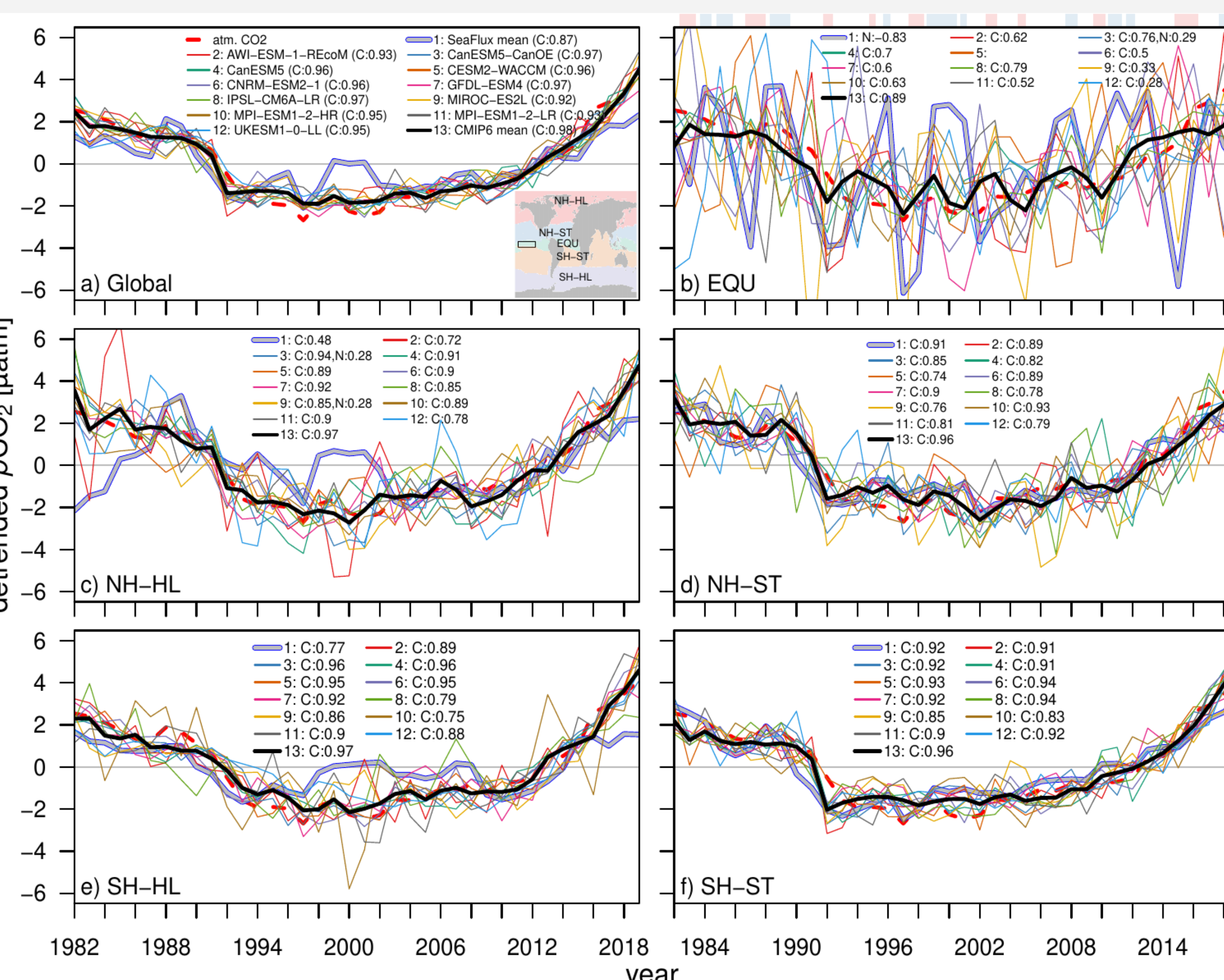
## Discrepancies in temporal $p\text{CO}_2$ variability from Earth System Models and $p\text{CO}_2$ -products related to high-latitude mixed layer dynamics and equatorial upwelling

Christopher Danek (cdanek@awi.de) and Judith Hauck

Alfred Wegener Institute for Polar and Marine Research (AWI), Am Handelshafen 12, Bremerhaven, 27570, Bremen, Germany

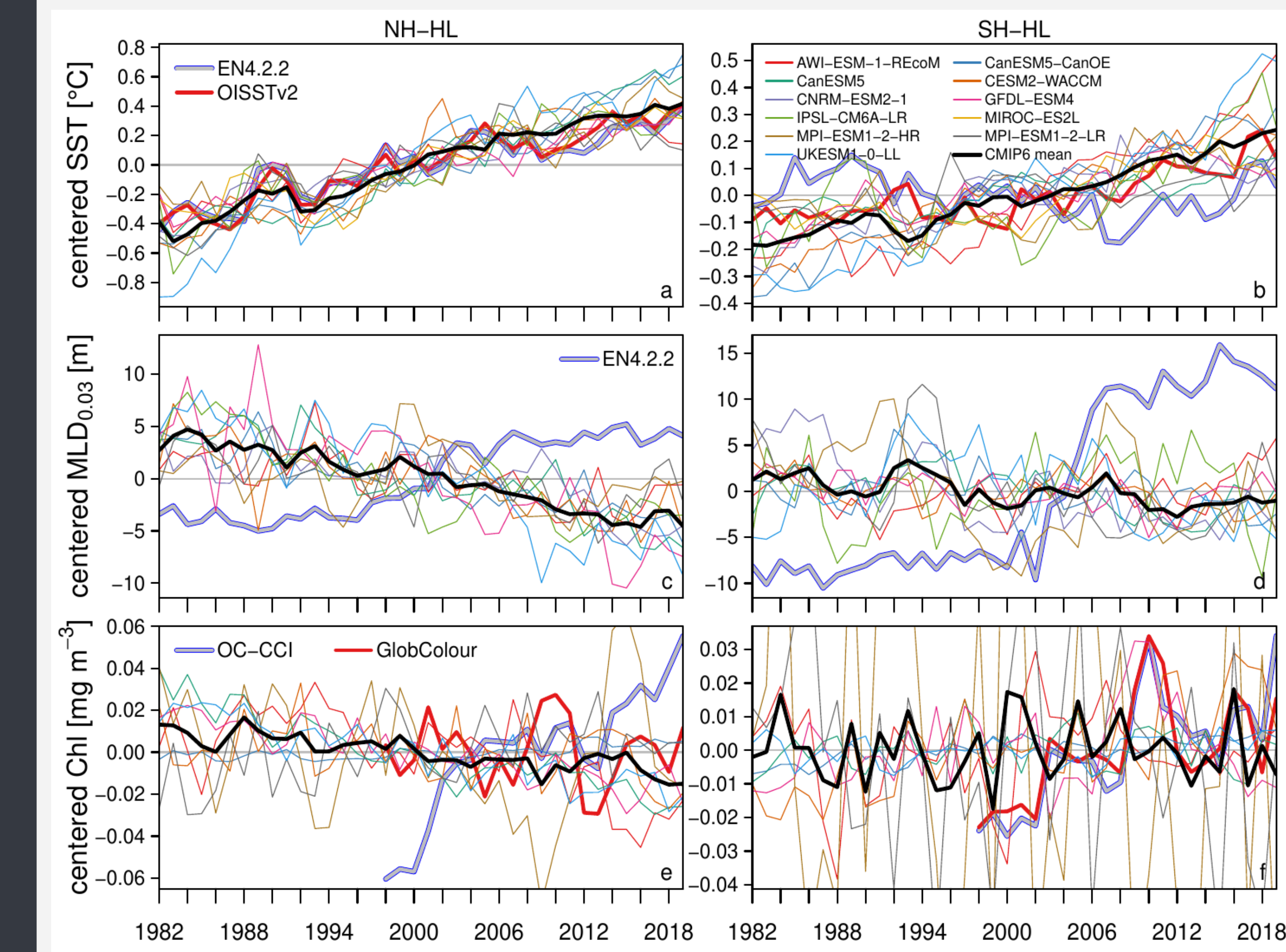
# But seawater $p\text{CO}_2$ variability is off in CMIP6 models in equatorial and high latitudes

The temporal variability of seawater  $p\text{CO}_2$  from the SeaFlux data product is largely determined by the atmospheric  $\text{CO}_2$  concentration (McKinley et al., 2017) and explains the slowdown and reinvigoration of  $F\text{CO}_2$  before and after the year 2000 (Gruber et al., 2023). This is especially the case in the subtropics of both hemispheres (NH-ST, SH-ST). The correlation, however, decreases in the high latitudes (NH-HL, SH-HL) and vanishes in the equatorial region (EQU).

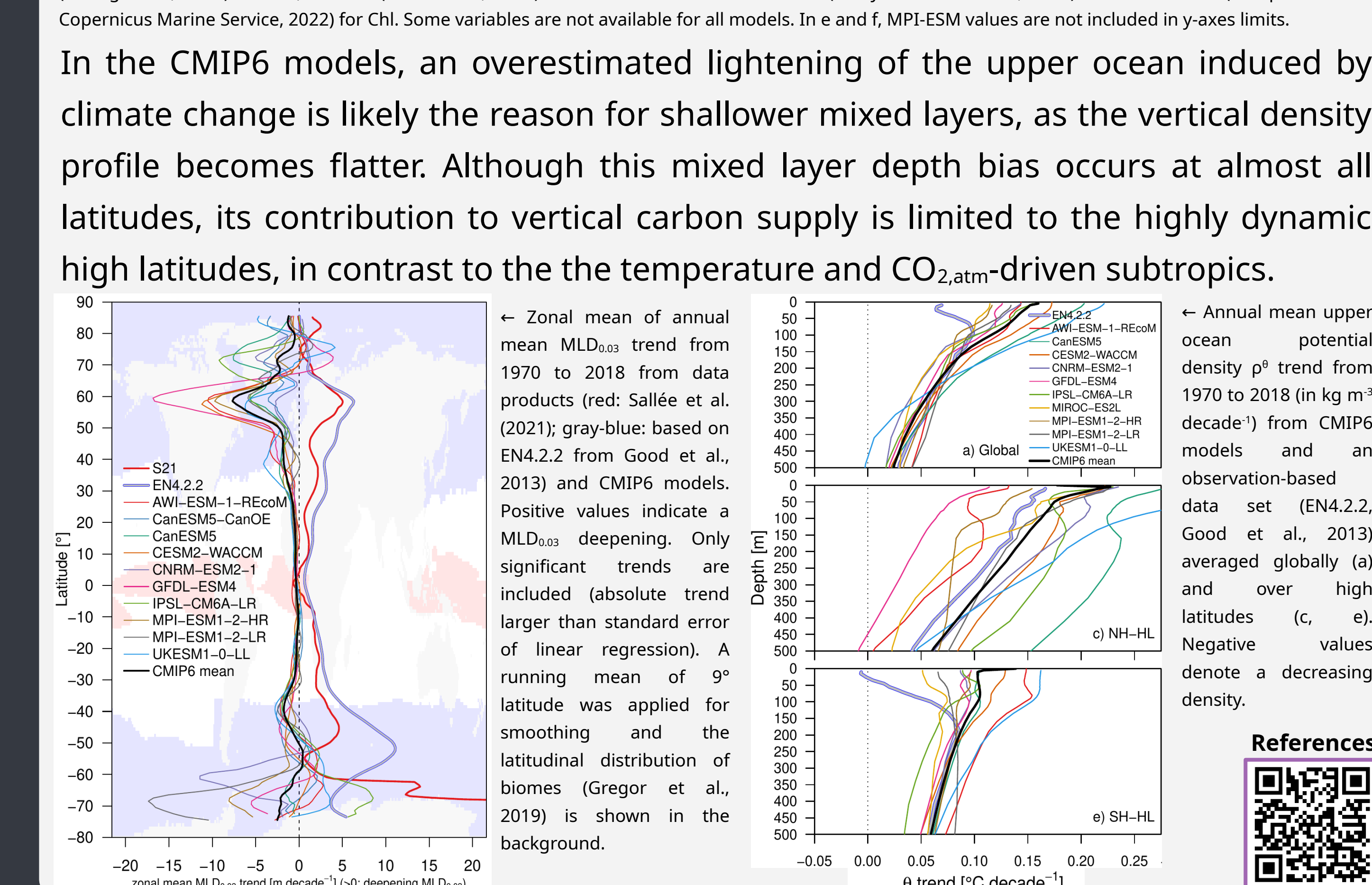


↑ Annual mean centered (1982–2019 mean removed) SST (top),  $\text{MLD}_{0.03}$  (middle) and Chl (bottom) from observational data sets and CMIP6 models, spatially averaged over NH-HL (left) and SH-HL biomes (right). Positive values indicate larger than the temporal mean (deeper for  $\text{MLD}_{0.03}$ ). Data sets are OISSTv2 (Huang et al., 2021) for SST, EN4.2.2 (Good et al., 2013) for SST and  $\text{MLD}_{0.03}$  and OC-CCI (Sathyendranath et al., 2019) and GlobColour (European Union-Copernicus Marine Service, 2022) for Chl. Some variables are not available for all models. In e and f, MPI-ESM values are not included in y-axes limits.

# Because all CMIP6 models show a shallowing mixed layer, in contrast to observations



↑ Zonal mean of annual mean  $\text{MLD}_{0.03}$  trend from 1970 to 2018 from data products (red: Sallée et al., 2021; gray-blue: based on EN4.2.2 from Good et al., 2013) and CMIP6 models. Positive values indicate a  $\text{MLD}_{0.03}$  deepening. Only significant trends are included (absolute trend larger than standard error of linear regression). A running mean of 9° latitude was applied for smoothing and the latitudinal distribution of biomes (Gregor et al., 2019) is shown in the background.



↑ Annual mean upper ocean potential density  $p^0$  trend from 1970 to 2018 ( $\text{kg m}^{-3} \text{decade}^{-1}$ ) from CMIP6 models and an observation-based data set (EN4.2.2, Good et al., 2013) averaged globally (a) and over high latitudes (c, e). Negative values denote a decreasing density.



References



ALFRED-WEGENER-INSTITUT  
HELMHOLTZ-ZENTRUM FÜR POLAR-  
UND MEERESFORSCHUNG

PI44D-1765